Journal of Power Sources 201 (2012) 267–273

Contents lists available at SciVerse ScienceDirect

Journal of Power Sources

journal homepage: www.elsevier.com/locate/jpowsour

Electrochemical performance of $Li_{3-x}Na_xV_2(PO_4)_3$/C composite cathode materials for lithium ion batteries

Quanqi Chen*, Xiaochang Qiao, Yaobin Wang, Tingting Zhang, Chang Peng, Wumei Yin, Li Liu

Key Laboratory of Environmentally Friendly Chemistry and Applications of Ministry of Education, School of Chemistry, Xiangtan University, Xiangtan, Hunan 411105, China

ARTICLE INFO

Article history:
Received 7 August 2011
Accepted 27 October 2011
Available online 6 November 2011

Keywords:
Lithium-ion batteries
Lithium vanadium phosphate
Galvanostatic intermittent titration technique
Sol–gel

ABSTRACT

The composites of monoclinic $Li_{3-x}Na_xV_2(PO_4)_3$ (x = 0, 0.03, 0.05 and 0.07) and carbon are prepared by a sol–gel method. The composites are investigated by X-ray diffraction (XRD), scanning electron microscopy (SEM), transmission electron microscopy (TEM) and electrochemical measurements. XRD results show that the cell volumes of the monoclinic Na-doped $Li_3V_2(PO_4)_3$ samples are larger than that of $Li_3V_2(PO_4)_3$. All Na-doped composites exhibit better electrochemical performance than that of pristine one and the $Li_{2.95}Na_{0.05}V_2(PO_4)_3$/C composite displays highest capacity and best cycle performance. The $Li_{2.95}Na_{0.05}V_2(PO_4)_3$/C composite presents initial capacities of 187 and 173.1 mAh g^{-1} at 0.2C and 1C between 3.0 and 4.8 V, respectively, much higher than that 175.5 mAh g^{-1} (0.2C) and 153.4 mAh g^{-1} (1C) of $Li_3V_2(PO_4)_3$/C composite. The capacity retentions of $Li_{2.95}Na_{0.05}V_2(PO_4)_3$/C are 95.3% and 91% at 0.2C and 1C after 30 cycles, respectively, while the capacity retentions of $Li_3V_2(PO_4)_3$/C are 90.4% and 87% at 0.2C and 1C after 30 cycles, respectively. The rapid Li^+ diffusion due to the doping of Na^+ is responsible for the good electrochemical performance of Na-doped $Li_3V_2(PO_4)_3$ cathode materials.

1. Introduction

The continuous searching for cathode materials that fulfill a variety of safety, environmental, cost and energy density demands promotes the advance of lithium ion batteries [1]. Compared with the oxide cathode materials such as $LiCoO_2$, $LiMn_2O_4$ and $LiNiO_2$, lithium metal phosphate compounds have been widely considered as promising next generation cathode materials for lithium-ion batteries because of their excellent thermal stability and cycle performance. Recently, monoclinic lithium vanadium phosphate ($Li_3V_2(PO_4)_3$) has received intensive attention as a cathode material because its high theoretical capacity (197 mAh g^{-1}), operating voltage and safety [2,3] are in favor of high power density and large scale applications. However, the lower intrinsic electronic conductivity (2×10^{-8} S cm^{-1}) [4] and cyclability restrict the wide applications of $Li_3V_2(PO_4)_3$. In order to overcome these restrictions, the addition of conductive materials such as carbon [2,3,5–17], Ag [18] and Cu [19] by solid-state, sol–gel, carbothermal reduction and hydrothermal methods was reported to improve the electronic conductivity and hence to enhance the electrochemical performance of $Li_3V_2(PO_4)_3$. The substitution of vanadium with alien ions such as Al^{3+} [20,21], Ti^{4+} [22], Ge^{4+} [23], Cr^{3+} [24], Co^{2+} [25], F^- [26], Mg^{2+} [27,28] and Mn^{2+} [29] has been recognized as an alternatively effective way to improve the cyclability and rate performance. However, to our knowledge, the effects of the doping alien ions except K^+ [30] in Li sites on the electrochemical performance of $Li_3V_2(PO_4)_3$ have been not investigated. Recently, the substitution of Li^+ by Na^+ was reported to improve the electrochemical performance of $LiFePO_4$ through improvement of Li^+ diffusion rate [31]. Moreover, $Na_3V_2(PO_4)_3$ has the NASICON ($Na_3Zr_2PSi_2O_{12}$) framework and allows Na^+ rapid diffusion in the interstitial space [32], and the radius of Li^+ (0.068 nm) is smaller than that of Na^+ (0.097 nm). Therefore, the substitution of Li^+ by a small amount of Na^+ may improve the diffusion rate of Li^+ and result in better electrochemical performance of $Li_3V_2(PO_4)_3$. In this work, we adopt a sol–gel method to prepare the $Li_{3-x}Na_xV_2(PO_4)_3$/C composite (x = 0.03, 0.05 and 0.07) to improve both electronic and ionic conductivity, and the effects of Na^+ doping in Li sites on the diffusion coefficient of Li^+ and the electrochemical performance of $Li_3V_2(PO_4)_3$ are investigated.

2. Experimental

$Li_{3-x}Na_xV_2(PO_4)_3$/C (x = 0, 0.03, 0.05 and 0.07) composites were prepared by a sol–gel method [33]. V_2O_5 powder was dissolved by 10% peroxide solution to form a clear orange solution. Citric acid equivalent mole to V_2O_5 and stoichiometric amount of $NH_4H_2PO_4$, LiOH and $NaNO_3$ were added to the above orange solution, and the mixed solution was aged with continuous stirring at 60 °C in a thermostatic bath for 10 h to get the green precursor gel. The obtained

* Corresponding author. Tel.: +86 731 58292206; fax: +86 731 58292251.
E-mail addresses: quanqi.chen@yahoo.com, qqchen@xtu.edu.cn (Q. Chen).

0378-7753/$ – see front matter © 2011 Elsevier B.V. All rights reserved.
doi:10.1016/j.jpowsour.2011.10.133

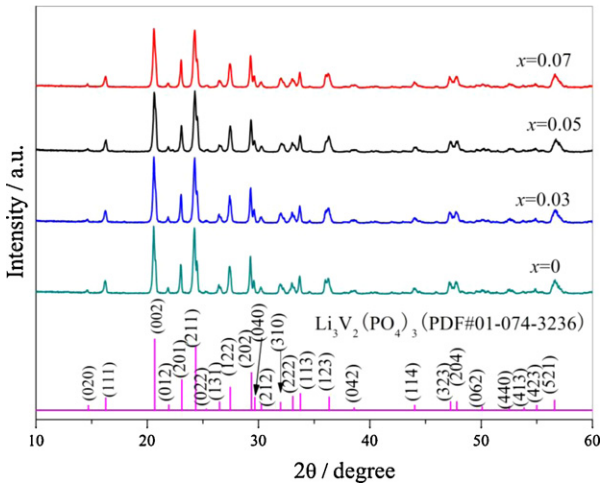

Fig. 1. XRD patterns of $Li_{3-x}Na_xV_2(PO_4)_3$/C samples (x = 0, 0.03, 0.05 and 0.07).

precursor gel was dried at 80 °C in a vacuum oven, pelletized and heated at 300 °C in a tubular furnace with following argon for 4 h to remove NH_3, H_2O and volatile compounds decomposed from the organic compounds. After cooling to room temperature, the resulted product was ground, pelletized and sintered at 800 °C for 8 h in argon atmosphere to yield black $Li_{3-x}Na_xV_2(PO_4)_3$/C composite.

The crystallinity and structure of the samples were characterized by a D/Max III X-ray diffractometer (XRD) with Cu Kα radiation (λ = 0.15418 nm). The carbon content of samples was determined by a carbon–sulfur analyzer (Mlti EA2000). The surface morphology of samples was observed using a JEOL JSM-6360 scanning electron microscopy (SEM) and a JEOL JEM2010 transmission electron microscopy (TEM).

The electrochemical tests of $Li_{3-x}Na_xV_2(PO_4)_3$/C samples were carried out using coin cells assembled in an argon-filled glove box. The cathodes consisted of $Li_{3-x}Na_xV_2(PO_4)_3$/C composite materials, polyvinylidene fluoride (PVDF) binder and acetylene black in a weight ratio of 80:10:10 and were assembled into 2032 size coin cells with lithium as counter electrode, Celgard 2400 separators and a 1 M $LiPF_6$ electrolyte solution in a mixture of ethylene carbonate (EC) and dimethyl carbonate (DMC) (1:1 in volume). In the cycling procedure, galvanostatic charge–discharge measurements were carried out in a Neware battery testing system (Neware, Shenzhen, China) and the cells were charged to 4.8 V and discharged to 3.0 V with different rates (1C = 197 mA g^{-1}). The electrochemical specific capacity of samples was calculated based on the mass of the active materials. For galvanostatic intermittent titration technique (GITT) measurement, a constant current flux of I_0 was applied for a known time followed by open circuit for a specific time. The measurements of electrochemical impedance spectroscopy (EIS) and cyclic voltammetry (CV) were conducted on an IM6ex electrochemistry workstation (Zahner-Elektrick, German).

3. Results and discussion

3.1. Physical characterization

The final products are black powders instead of green pristine $Li_3V_2(PO_4)_3$ [4] because of existence of residual carbon, and the carbon content was determined by carbon–sulfur analyzer. The XRD patterns of the final products are shown in Fig. 1 and all diffraction peaks can be indexed by well-defined monoclinic phase, consistent with monoclinic $Li_3V_2(PO_4)_3$ (PDF 01-074-3236). Absence of diffraction peaks of impurity suggests that the final products are composites of monoclinic phase and carbon, indicating that doping a low amount of Na^+ does not significantly affect the monoclinic structure of $Li_3V_2(PO_4)_3$. The composites are $Li_3V_2(PO_4)_3$/C, $Li_{2.97}Na_{0.03}V_2(PO_4)_3$/C, $Li_{2.95}Na_{0.05}V_2(PO_4)_3$/C and $Li_{2.93}Na_{0.07}V_2(PO_4)_3$/C, respectively, and the carbon contents of the corresponding composites are 3.10, 2.98, 2.90 and 2.95 wt.%, respectively. The cell parameters were calculated by Jade 5.0, an XRD analysis software, and the cell parameters are listed in Table 1. The results reveal that cell parameters change slightly with the increase of Na content and the cell volumes of Na-doped $Li_3V_2(PO_4)_3$ samples are somewhat larger than that of pristine one, the substitution of smaller radius of Li^+ (r = 0.068 nm) by larger Na^+ (r = 0.097 nm) may be responsible for the variation. Larger cell volume could supply the larger channel for transport of Li^+ and facilitate rapid diffusion of Li^+ in particles of active materials, in favor of improving the electrochemical performance of $Li_{3-x}Na_xV_2(PO_4)_3$/C composites.

SEM images of $Li_3V_2(PO_4)_3$/C, $Li_{2.97}Na_{0.03}V_2(PO_4)_3$/C, $Li_{2.95}Na_{0.05}V_2(PO_4)_3$/C and $Li_{2.93}Na_{0.07}V_2(PO_4)_3$/C composites are shown in Fig. 2a–d, respectively, and all composites consist of fine particles with coarser surface. Typical TEM and HRTEM images of $Li_{2.95}Na_{0.05}V_2(PO_4)_3$/C composite are presented in Fig. 2e and f, respectively, and Fig. 2e and f reveal that the coarser surface is composed of rough and porous amorphous carbon and the active material is covered by amorphous carbon. The porous amorphous carbon could improve the electronic conductivity of active material, suppress the growth of pristine and Na-doped $Li_3V_2(PO_4)_3$ particles and not impede the diffusion of lithium ion from the surface of active material to electrolyte, resulting in the improved electrochemical performance of pristine and Na-doped $Li_3V_2(PO_4)_3$ samples.

3.2. Electrochemical measurements

Fig. 3a and b depicts the initial charge/discharge profiles and cycle performance of $Li_{3-x}Na_xV_2(PO_4)_3$/C (x = 0, 0.03, 0.05 and 0.07) composites at 0.2C (39.4 mA g^{-1}) in the voltage range of 3.0–4.8 V, respectively. Fig. 3a reveals that all above-mentioned composites exhibit four charge plateaus and three discharge ones, similar to that of the $Li_3V_2(PO_4)_3$/C composite in the previous reports [2,3,5–10,17–19,33,34]. It is clear that the discharge capacities of $Li_{3-x}Na_xV_2(PO_4)_3$/C composites increase from 175.5 mAh g^{-1} (x = 0) to 181.3 mAh g^{-1} (x = 0.03) and 187 mAh g^{-1} (x = 0.05), and then decrease to 179.3 mAh g^{-1} (x = 0.07), suggesting that the substitution of Li^+ by Na^+ is in favor of improving the discharge capacity of $Li_3V_2(PO_4)_3$ in our experiment. This may be mainly due to the fact that the substitution of larger radius of Na^+ enlarges the cell volume of pristine $Li_3V_2(PO_4)_3$ and results in larger channel for rapid diffusion of Li^+ in active material, in favor of reducing the polarization during the processes of Li^+ insertion and extraction and improving the electrochemical performance of $Li_3V_2(PO_4)_3$/C composite. Amongst all $Li_{3-x}Na_xV_2(PO_4)_3$/C (x = 0, 0.03, 0.05 and 0.07) composites, the $Li_{2.95}Na_{0.05}V_2(PO_4)_3$/C composite shows highest discharge capacity of 187 mAh g^{-1}, higher than the previous pristine or doped $Li_3V_2(PO_4)_3$ [2,6,7,9,10,18–20,24,25,29,33] and close to the theoretical capacity of 197 mAh g^{-1}, indicating that the doped Na^+ content of x = 0.05 is optimal. Fig. 3b illustrates that all above-mentioned composites exhibit better cycle performance. After 30 cycles, the capacity retention rates of $Li_{3-x}Na_xV_2(PO_4)_3$/C composites with x = 0, 0.03, 0.05 and 0.07 are 90.4%, 92.3%, 95.3% and 94.2%, respectively, implying that the doped Na^+ may effectively enhance the stability of $Li_3V_2(PO_4)_3$ and improve the cycle performance. It is noted that $Li_{2.95}Na_{0.05}V_2(PO_4)_3$/C displays best cycle performance amongst the above-mentioned four composites and exhibits highest discharge capacity of 178.2 mAh g^{-1} after 30 cycles, while the

Table 1
Lattice parameters of the $Li_{3-x}Na_xV_2(PO_4)_3$ ($x = 0$, 0.03, 0.05 and 0.07) samples.

Samples	a (nm)	b (nm)	c (nm)	β (°)	Cell volume (nm^3)
$Li_3V_2(PO_4)_3$	0.8615	1.2058	0.8616	90.5	0.8950
$Li_{2.97}Na_{0.03}(PO_4)_3$	0.8635	1.2070	0.8596	90.3	0.8959
$Li_{2.95}Na_{0.05}(PO_4)_3$	0.8658	1.2079	0.8580	90.4	0.8973
$Li_{2.93}Na_{0.07}(PO_4)_3$	0.8668	1.2072	0.8573	90.3	0.8971

discharge capacity of pristine $Li_3V_2(PO_4)_3$/C after 30 cycles is only 158.7 mAh g^{-1}.

Fig. 4 shows the initial charge/discharge profiles and cycle performance of $Li_{3-x}Na_xV_2(PO_4)_3$/C ($x = 0$, 0.03, 0.05 and 0.07) composites at 1*C* in the voltage range of 3.0–4.8 V. As shown in Fig. 4a, the initial discharge capacities of $Li_3V_2(PO_4)_3$/C, $Li_{2.97}Na_{0.03}V_2(PO_4)_3$/C, $Li_{2.95}Na_{0.05}V_2(PO_4)_3$/C and $Li_{2.93}Na_{0.07}V_2(PO_4)_3$/C are 153.4, 160.5, 173.1 and 156.4 mAh g^{-1}, respectively, smaller than that of corresponding composites at 0.2*C* due to the higher polarization at larger current density.

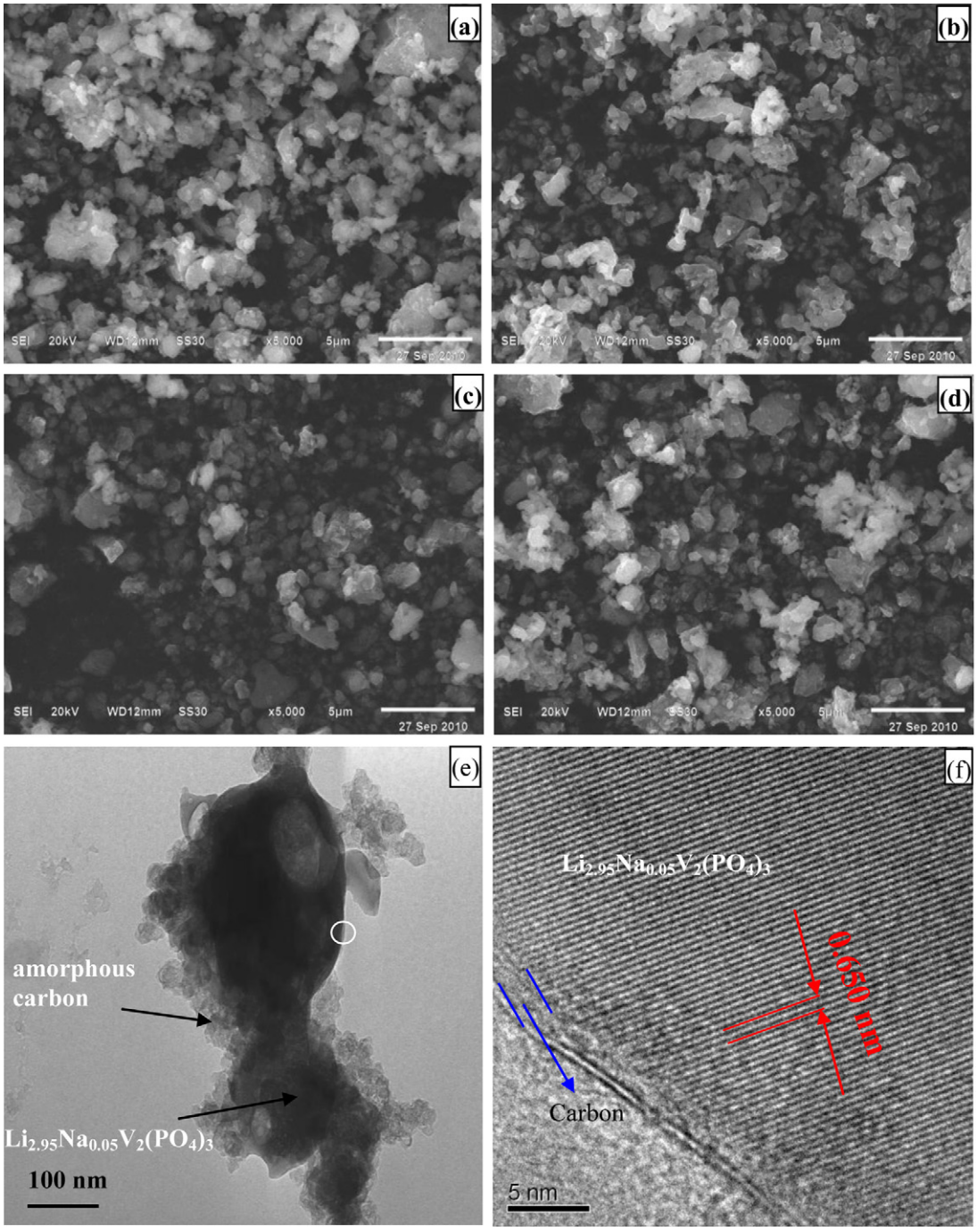

Fig. 2. SEM images of $Li_{3-x}Na_xV_2(PO_4)_3$/C composites: (a) $x = 0$, (b) $x = 0.03$, (c) $x = 0.05$ and (d) $x = 0.07$; TEM image (e) and HRTEM image (f) of $Li_{2.95}Na_{0.05}V_2(PO_4)_3$/C composite.

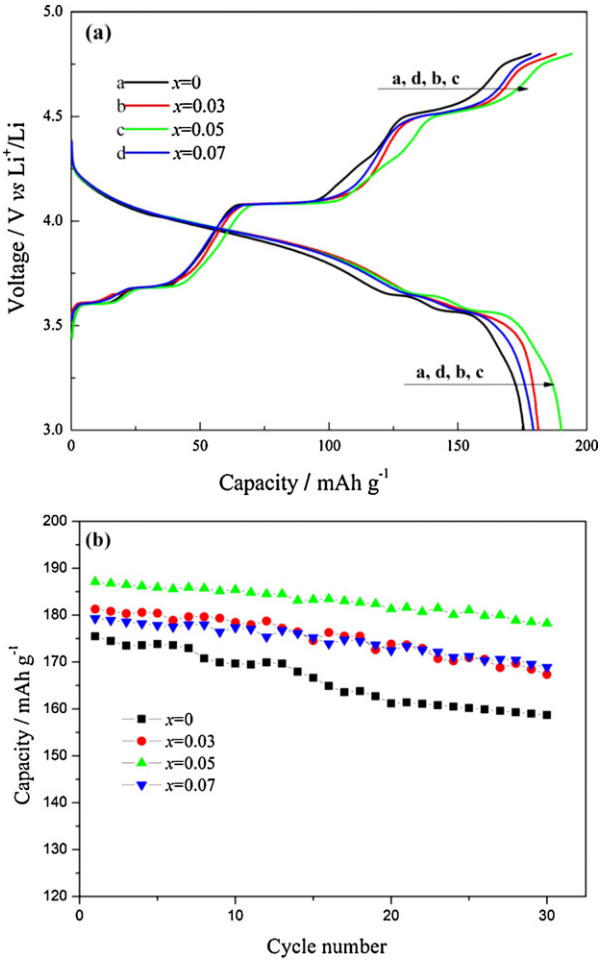

Fig. 3. Initial charge/discharge profiles (a) and cycle performance (b) of $Li_{3-x}Na_xV_2(PO_4)_3$/C composites (x = 0, 0.03, 0.05 and 0.07) at 0.2*C* in the voltage range of 3.0–4.8 V.

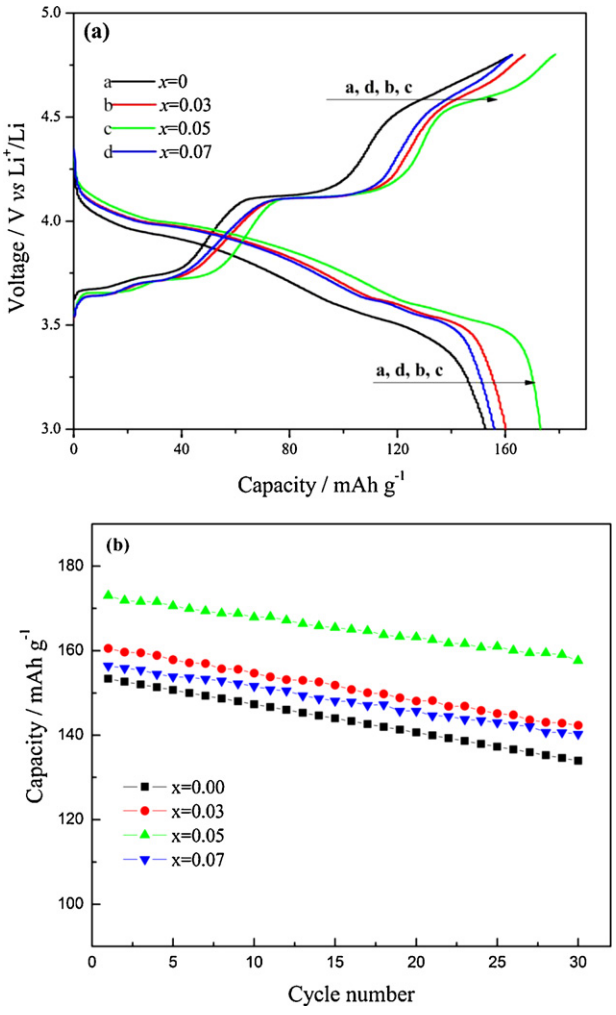

Fig. 4. Initial charge/discharge profiles (a) and cycle performance (b) of $Li_{3-x}Na_xV_2(PO_4)_3$/C composites at 1*C* in the voltage range of 3.0–4.8 V.

Amongst all the composites, $Li_{2.95}Na_{0.05}V_2(PO_4)_3$/C presents highest discharge capacity and smallest voltage difference of charge and discharge plateaus, indicating that $Li_{2.95}Na_{0.05}V_2(PO_4)_3$/C composite has lowest electrochemical polarization and leads to better reversibility in the charge–discharge processes. Fig. 4b reveals that the four composites still remain better cyclability at higher current density of 1*C*, which may be attributed to the excellent structure stability of pristine and Na-doped monoclinic $Li_3V_2(PO_4)_3$. $Li_{2.95}Na_{0.05}V_2(PO_4)_3$/C composite has best cyclability and highest discharge capacity amongst the four composites, and exhibits capacity retention of 91% and still remains capacity of 158.2 mAh g^{-1} after 30 cycles at 1*C*, while the capacity retention rates of $Li_3V_2(PO_4)_3$/C, $Li_{2.97}Na_{0.03}V_2(PO_4)_3$/C and $Li_{2.93}Na_{0.07}V_2(PO_4)_3$/C after 30 cycles at 1*C* are 87%, 89% and 90%, respectively. The above results show that the doping of Na^+ facilitates the improvement of capacity and cycle performance of $Li_3V_2(PO_4)_3$.

In order to investigate the electrochemical behavior of $Li_{3-x}Na_xV_2(PO_4)_3$/C composites in the processes of charge and discharge, cyclic voltammetry (CV) was carried out in the potential range of 3.0–5.0 V at a scanning rate of 0.1 mV s^{-1}, and the results are presented in Fig. 5. As can be seen, all the four composites exhibit four anodic peaks, labeled as a_1, a_2, a_3 and a_4, and three cathodic peaks, denoted as c_1, c_2 and c_3, in consistence with the charge and discharge voltage plateaus of composites in Figs. 3a and 4a, indicating that Na^+ doping does not change the electrochemical reaction mechanism of $Li_3V_2(PO_4)_3$. The potentials for the CV peaks of $Li_{3-x}Na_xV_2(PO_4)_3$/C composites are listed in Table 2. The results show that the potentials of anodic peaks of Na-doped $Li_3V_2(PO_4)_3$ are lower than that of pristine $Li_3V_2(PO_4)_3$, while the potentials of cathodic peaks of Na-doped $Li_3V_2(PO_4)_3$ are higher than that of pristine $Li_3V_2(PO_4)_3$, suggesting that extraction and insertion of Li^+ in Na-doped $Li_3V_2(PO_4)_3$ composites need lower energy than that of pristine $Li_3V_2(PO_4)_3$ and Na^+ doping facilitates

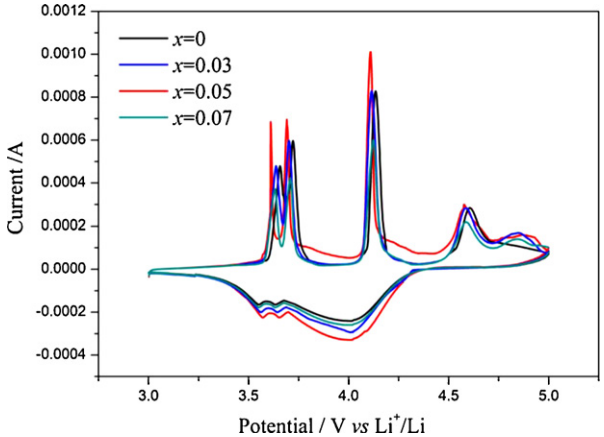

Fig. 5. Cyclic voltammograms of $Li_{3-x}Na_xV_2(PO_4)_3$/C composites at a scanning rate of 0.1 mV s^{-1} in the potential range of 3.0–5.0 V.

Table 2
Potentials for CV peaks of $Li_{3-x}Na_xV_2(PO_4)_3$/C composites.

Sample	a_1 (V)	a_2 (V)	a_3 (V)	a_4 (V)	c_1 (V)	c_2 (V)	c_3 (V)
$Li_3V_2(PO_4)_3$/C	3.657	3.720	4.135	4.606	3.998	3.634	3.55
$Li_{2.97}Na_{0.03}V_2(PO_4)_3$/C	3.637	3.702	4.115	4.586	4.009	3.644	3.561
$Li_{2.95}Na_{0.05}V_2(PO_4)_3$/C	3.615	3.691	4.108	4.578	4.018	3.653	3.572
$Li_{2.93}Na_{0.07}V_2(PO_4)_3$/C	3.632	3.709	4.123	4.590	4.010	3.635	3.552

Table 3
The fitting results of Nyquist plots for $Li_{3-x}Na_xV_2(PO_4)_3$/C composites.

$Li_{3-x}Na_xV_2(PO_4)_3$/C	$x=0$	$x=0.03$	$x=0.05$	$x=0.07$
R_s (ohm)	3.08	2.74	2.55	2.65
R_{ct} (ohm)	495.3	202.3	133.1	248.4

improvement of electrochemical performance of $Li_3V_2(PO_4)_3$. The potential differences between anodic and cathodic peaks of Na-doped $Li_3V_2(PO_4)_3$ are smaller than that of pristine $Li_3V_2(PO_4)_3$, which reveals that Na-doped $Li_3V_2(PO_4)_3$/C composites have better reversibility than that of $Li_3V_2(PO_4)_3$. Amongst the three Na-doped $Li_3V_2(PO_4)_3$/C composites, the $Li_{2.95}Na_{0.05}V_2(PO_4)_3$/C composite has the smallest potential difference of anodic and cathodic peaks, implying that $Li_{2.95}Na_{0.05}V_2(PO_4)_3$/C has best reversibility and electrochemical performance, in accordance with the electrochemical performance of composites (Figs. 3 and 4).

The impedance behaviors of $Li_{3-x}Na_xV_2(PO_4)_3$/C composites are depicted in Fig. 6 and all composites exhibit typical Nyquist characteristics. An intercept in the high frequency region of the Z' real axis corresponds to the ohmic resistance (R_s), the combined resistance of the electrolyte and the contacts of the cell. The semicircle in high-middle frequency region indicates the charge transfer process on the electrode interface, revealing the lithium transfer rate parameters as well as the capacitance of the SEI (solid electrolyte interface)/electrolyte double-layer. The inclined line in the lower frequency region represents the Warburg impedance (Z_w), which is associated with the diffusion of Li^+ in $Li_{3-x}Na_xV_2(PO_4)_3$ particles. The constant phase element (CPE) stands for the double layer capacitance. The plots were fitted using the equivalent circuit, which is shown in the inset of Fig. 6, and the fitting result (Table 3) reveals that the charge transfer resistance (R_{ct}) of Na-doped $Li_3V_2(PO_4)_3$ composites is lower than that of pristine $Li_3V_2(PO_4)_3$. The smaller R_{ct} is in favor of rapid electrochemical reaction and may result in better electrochemical performance of the active materials, and the smallest R_{ct} for $Li_{2.95}Na_{0.05}V_2(PO_4)_3$/C composite indicates that $Li_{2.95}Na_{0.05}V_2(PO_4)_3$/C has the best electrochemical performance amongst the four composites, in agreement with the results (Figs. 3 and 4).

It is well known that electrochemical performance of intercalation cathode materials is mainly controlled by the kinetics of Li^+ extraction and insertion and the diffusion of Li^+ in electroactive particles is a key factor to influence the kinetics of Li^+ extraction/insertion. In order to investigate the effect of Na^+ doping on the diffusion coefficient of Li^+, D_{Li^+}, comparative study on the diffusion coefficient of Li^+ in $Li_3V_2(PO_4)_3$/C and $Li_{2.95}Na_{0.05}V_2(PO_4)_3$/C was carried out. The diffusion coefficient of Li^+ was determined by GITT method and D_{Li^+} was calculated by the following equation [35,36]:

$$D_{Li^+} = \frac{4}{\pi}\left(\frac{m_B V_m}{M_B S}\right)^2 \left(\frac{\Delta E_S}{\tau(dE_\tau/\sqrt{\tau})}\right)^2 \quad \left(\tau \ll \frac{l^2}{D_{Li^+}}\right) \tag{1}$$

where m_B, M_B and V_m are the mass, molecular weight and molar volume of the electroactive compound, respectively. S is the total area of contact between the electrolyte and the electrode. τ is the time period of charge or discharge at a constant current of I_0, and l is the thickness of the electrode. ΔE_s is the difference in open circuit voltage measured at the end of two sequential open-circuit relaxation steps, and E_τ is the cell voltage during charging or discharging at the time of current of flux. If there is a linear correlation of E_τ with $\tau^{1/2}$, Eq. (1) is further simplified to Eq. (2) [35,36]:

$$D_{Li^+} = \frac{4}{\pi\tau}\left(\frac{m_B V_m}{M_B S}\right)^2 \left(\frac{\Delta E_S}{\Delta E_\tau}\right)^2 \quad \left(\tau \ll \frac{l^2}{D_{Li^+}}\right) \tag{2}$$

Fig. 7 shows the GITT curves for the second charge/discharge cycle of $Li_3V_2(PO_4)_3$/C and $Li_{2.95}Na_{0.05}V_2(PO_4)_3$/C. GITT test was performed by charging/discharging the cell for an interval of 10 min at a galvanostatic current of 0.18 mA (corresponding to about 0.1C), relaxing 40 min to approach nearly equilibrium state and repeating this process again until the voltage window of operation, 3.0–4.8 V. GITT curves indicate that overall time of the charging or discharging process of $Li_{2.95}Na_{0.05}V_2(PO_4)_3$/C is longer than that of $Li_3V_2(PO_4)_3$/C, suggesting that capacity of $Li_{2.95}Na_{0.05}V_2(PO_4)_3$/C is

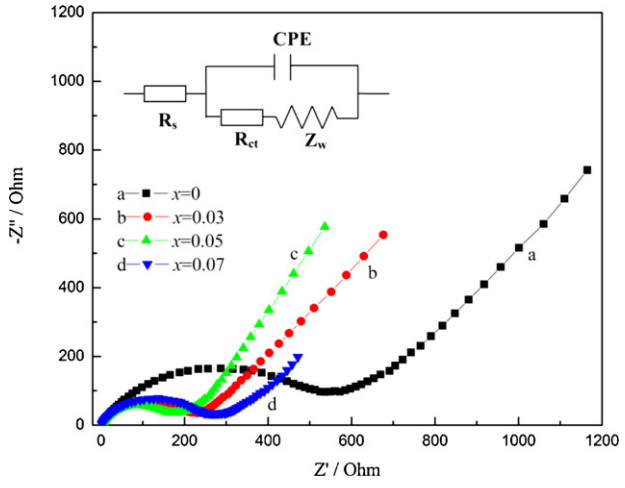

Fig. 6. Nyqusit plots of $Li_{3-x}Na_xV_2(PO_4)_3$/C composites after initial charged to 4.8 V. Equivalent circuit used for curve fitting is shown inset.

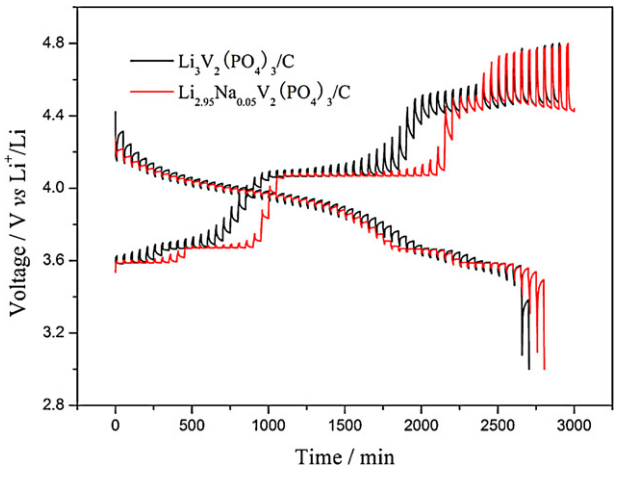

Fig. 7. GITT curves for the second charge/discharge cycle of $Li_3V_2(PO_4)_3$/C and $Li_{2.95}Na_{0.05}V_2(PO_4)_3$/C in the voltage window of 3.0–4.8 V.

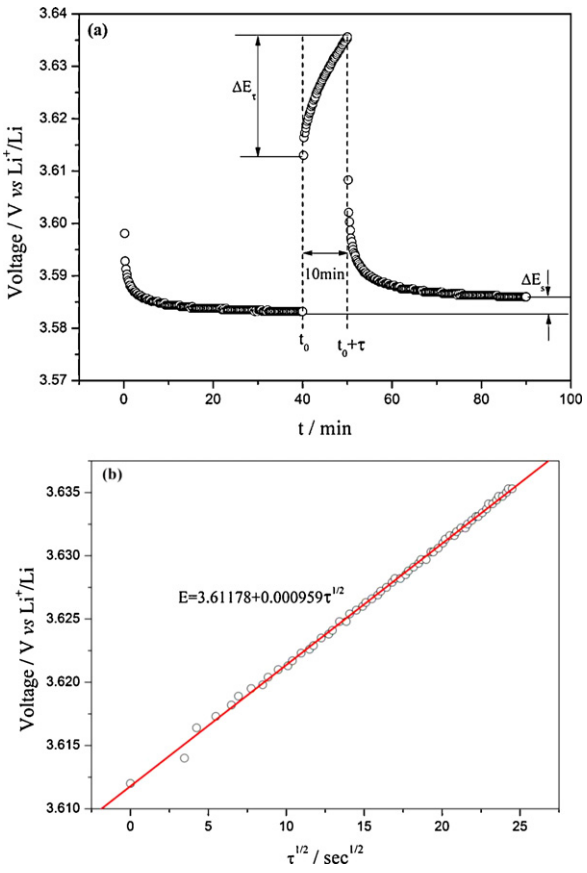

Fig. 8. Applied current pulse *vs* voltage profile for a single titration at 3.58 V during charge for $Li_3V_2(PO_4)_3$/C with schematic representation of different profile parameters (a) and variation of cell voltage for the above titration plotted against $\tau^{1/2}$ to show the linear fitting (b).

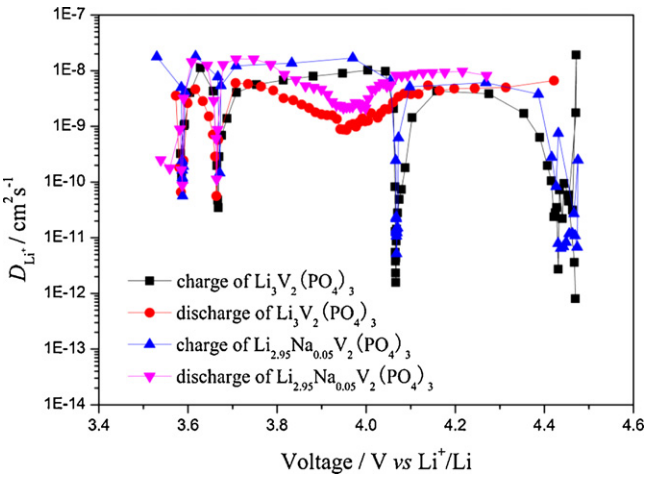

Fig. 9. The Li^+ diffusion coefficients of $Li_3V_2(PO_4)_3$/C and $Li_{2.95}Na_{0.05}V_2(PO_4)_3$/C electrodes calculated from GITT curves as a function of cell voltage during processes of charge and discharge.

higher than that of $Li_3V_2(PO_4)_3$/C, in consistence with the results (Figs. 3 and 4). A single step of GITT at 3.58 V during the charge process is depicted in Fig. 8a with schematic labeling of different parameters. Fig. 8b reveals that the variation of cell voltage during the above titration step shows a straight line behavior against $\tau^{1/2}$, therefore, the value of D_{Li^+} was conveniently calculated by Eq. (2) in our experiment. However, the calculation of D_{Li^+} is based on the assumption that the possible change in molar volume (V_m) of electroactive materials during the processes of Li^+ extraction and insertion is ignored and V_m is considered as a constant. The V_m is calculated based on the cell volumes (Table 1), and the V_m for $Li_3V_2(PO_4)_3$ and $Li_{2.95}Na_{0.05}V_2(PO_4)_3$ is 134.70 and 135.04 $cm^3\ mol^{-1}$, respectively. The Li^+ diffusion coefficients of $Li_3V_2(PO_4)_3$/C and $Li_{2.95}Na_{0.05}V_2(PO_4)_3$/C calculated from GITT curves as a function of cell voltage during cycling are presented in Fig. 9. Both $Li_3V_2(PO_4)_3$/C and $Li_{2.95}Na_{0.05}V_2(PO_4)_3$/C display four minima of D_{Li^+} in the charge process as well as three minima in the discharge process, and the minima correspond to the voltage plateaus of charge–discharge and the CV peak potentials. A similar minimum in the D_{Li^+} *vs* voltage plots was observed in $Li_3V_2(PO_4)_3$ [36]. In the process of Li^+ extraction, the D_{Li^+} values of $Li_3V_2(PO_4)_3$/C are in the scope of 4.48×10^{-12}–$1.32 \times 10^{-8}\ cm^2\ s^{-1}$ except for the fourth minimum $5.12 \times 10^{-13}\ cm^2\ s^{-1}$, similar to the result reported by Rui et al. [36], while D_{Li^+} values of $Li_{2.95}Na_{0.05}V_2(PO_4)_3$/C are in the range of 1.56×10^{-11}–$5.41 \times 10^{-8}\ cm^2\ s^{-1}$ except for the fourth minimum $1.25 \times 10^{-12}\ cm^2\ s^{-1}$. In the process of Li^+ insertion, D_{Li^+} values of $Li_3V_2(PO_4)_3$/C and $Li_{2.95}Na_{0.05}V_2(PO_4)_3$/C are in the range of 6.61×10^{-11}–6.03×10^{-9} and 2.63×10^{-10}–$4.86 \times 10^{-8}\ cm^2\ s^{-1}$, respectively. Further comparative study of D_{Li^+} values shown in Fig. 9 reveals that Li^+ diffusion coefficients of $Li_{2.95}Na_{0.05}V_2(PO_4)_3$/C are at least three times higher than that of $Li_3V_2(PO_4)_3$/C at the corresponding voltage, suggesting that $Li_{2.95}Na_{0.05}V_2(PO_4)_3$/C is more favorable than $Li_3V_2(PO_4)_3$/C to rapid diffusion of lithium ion and rapid diffusion of lithium ion may result in better electrochemical performance of electroactive materials.

4. Conclusions

The $Li_{3-x}Na_xV_2(PO_4)_3$/C ($x = 0$, 0.03, 0.05 and 0.07) composites have been successfully prepared by a sol–gel method using citric acid as both a chelating agent and carbon sources, and $NaNO_3$ as Na^+ sources. XRD results reveal that a single monoclinic phase of pristine or Na-doped $Li_3V_2(PO_4)_3$ was obtained and a lower concentration of doped Na^+ does not significantly change the monoclinic structure of $Li_3V_2(PO_4)_3$. The cell volume of Na-doped $Li_3V_2(PO_4)_3$ is somewhat larger than that of pristine one. Typical TEM images of $Li_{2.95}Na_{0.05}V_2(PO_4)_3$/C indicate that monoclinic $Li_{2.95}Na_{0.05}V_2(PO_4)_3$ is covered by porous and amorphous carbon. The Na-doped $Li_3V_2(PO_4)_3$/C composites display much better electrochemical performance than that of $Li_3V_2(PO_4)_3$/C and $Li_{2.95}Na_{0.05}V_2(PO_4)_3$/C exhibits the highest capacity and best cycle performance amongst the four composites. In the voltage range of 3.0–4.8 V, $Li_{2.95}Na_{0.05}V_2(PO_4)_3$/C exhibits the highest initial capacity of 187 mAh g^{-1} at 0.2*C*, much higher than that of 175.5 mAh g^{-1} of $Li_3V_2(PO_4)_3$/C. Even at 1*C* $Li_{2.95}Na_{0.05}V_2(PO_4)_3$/C shows initial capacity of 173.1 mAh g^{-1} and capacity retention of 91% after 30 cycles, while $Li_3V_2(PO_4)_3$/C displays lower capacity of 133.5 mAh g^{-1} after 30 cycles. The comparative study on the Li^+ diffusion coefficients of $Li_3V_2(PO_4)_3$/C and $Li_{2.95}Na_{0.05}V_2(PO_4)_3$/C indicates that substitution of Li^+ with a suitable amount of Na^+ could facilitate to improve the diffusion rate of Li^+ and result in high capacity and cycle performance. The substitution of Li^+ by larger radius ions may be an effective way to improve the electrochemical performance of other intercalation cathode materials.

Acknowledgement

The authors gratefully acknowledge financial support from the Scientific Research Fund of Hunan Provincial Education Department (No. 09C947), National University Student Innovative Project of China (No. 101053015) and the NSFC (No. 20871101).

References

[1] J.-M. Tarascon, M. Armand, Nature 414 (2001) 359–367.
[2] M.Y. Saidi, J. Barker, H. Huang, J.L. Swoyer, G. Adamson, Electrochem. Solid-State Lett. 5 (2002) A149–A151.
[3] H. Huang, S.-C. Yin, T. Kerr, N. Taylor, L.F. Nazar, Adv. Mater. 14 (2002) 1525–1528.
[4] S.C. Yin, H. Grondey, P. Strobel, M. Anne, L.F. Nazar, J. Am. Chem. Soc. 125 (2003) 10402–10411.
[5] P. Fu, Y. Zhao, Y. Dong, X. An, G. Shen, J. Power Sources 162 (2006) 651–657.
[6] Y. Li, Z. Zhou, M. Ren, X. Gao, J. Yan, Electrochim. Acta 51 (2006) 6498–6502.
[7] P. Fu, Y. Zhao, X. An, Y. Dong, X. Hou, Electrochim. Acta 52 (2007) 5281–5285.
[8] Y. Li, Z. Zhou, X. Gao, J. Yan, Electrochim. Acta 52 (2007) 4922–4926.
[9] C. Chang, J. Xiang, X. Shi, X. Han, L. Yuan, J. Sun, Electrochim. Acta 53 (2008) 2232–2237.
[10] C.X. Chang, J.F. Xiang, X.X. Shi, X.Y. Han, L.J. Yuan, J.T. Sun, Electrochim. Acta 54 (2008) 623–627.
[11] M.M. Ren, Z. Zhou, X.P. Gao, W.X. Peng, J.P. Wei, J. Phys. Chem. C 112 (2008) 5689–5693.
[12] F. Yu, J.J. Zhang, Y.F. Yang, G.Z. Song, J. Inorg. Mater. 24 (2009) 349–352.
[13] J.-C. Zheng, X.-H. Li, Z.-X. Wang, H.-J. Guo, Q.-Y. Hu, W.-J. Peng, J. Power Sources 189 (2009) 476–479.
[14] T. Jiang, W.C. Pan, J. Wang, X.F. Bie, F. Du, Y.J. Wei, C.Z. Wang, G. Chen, Electrochim. Acta 55 (2010) 3864–3869.
[15] A. Pan, J. Liu, J.-G. Zhang, W. Xu, G. Cao, Z. Nie, B.W. Arey, S. Liang, Electrochem. Commun. 12 (2010) 1674–1677.
[16] L. Wang, L.-C. Zhang, I. Lieberwirth, H.-W. Xu, C.-H. Chen, Electrochem. Commun. 12 (2010) 52–55.
[17] Y.Q. Qiao, X.L. Wang, J.Y. Xiang, D. Zhang, W.L. Liu, J.P. Tu, Electrochim. Acta 56 (2011) 2269–2275.
[18] L. Zhang, X.L. Wang, J.Y. Xiang, Y. Zhou, S.J. Shi, J.P. Tu, J. Power Sources 195 (2010) 5057–5061.
[19] T. Jiang, Y.J. Wei, W.C. Pan, Z. Li, X. Ming, G. Chen, C.Z. Wang, J. Alloys Compd. 488 (2009) L26–L29.
[20] J. Barker, R.K.B. Gover, P. Burns, A. Bryan, J. Electrochem. Soc. 154 (2007) A307–A313.
[21] D. Ai, K. Liu, Z. Lu, M. Zou, D. Zeng, J. Ma, Electrochim. Acta 56 (2011) 2823–2827.
[22] S.Q. Liu, S.C. Li, K.L. Huang, Z.H. Chen, Acta Phys.-Chim. Sin. 23 (2007) 537–542.
[23] S.Q. Liu, S.C. Li, K.L. Huang, B.L. Gong, G. Zhang, J. Alloys Compd. 450 (2008) 499–504.
[24] Y. Chen, Y. Zhao, X. An, J. Liu, Y. Dong, L. Chen, Electrochim. Acta 54 (2009) 5844–5850.
[25] Q. Kuang, Y.M. Zhao, X.N. An, J.M. Liu, Y.Z. Dong, L. Chen, Electrochim. Acta 55 (2010) 1575–1581.
[26] S.K. Zhong, L.T. Liu, J.Q. Liu, J. Wang, J.W. Yang, Solid State Commun. 149 (2009) 1679–1683.
[27] C.S. Dai, Z.Y. Chen, H.Z. Jin, X.G. Hu, J. Power Sources 195 (2010) 5775–5779.
[28] J.S. Huang, L. Yang, K.Y. Liu, Y.F. Tang, J. Power Sources 195 (2010) 5013–5018.
[29] M. Bini, S. Ferrari, D. Capsoni, V. Massarotti, Electrochim. Acta 56 (2011) 2648–2655.
[30] Y.G. Mateyshina, N.F. Uvarov, J. Power Sources 196 (2011) 1494–1497.
[31] X. Yin, K. Huang, S. Liu, H. Wang, H. Wang, J. Power Sources 195 (2010) 4308–4312.
[32] J. Gopalakrishnan, K.K. Rangan, Chem. Mater. 4 (1992) 745–747.
[33] Q. Chen, J. Wang, Z. Tang, W. He, H. Shao, J. Zhang, Electrochim. Acta 52 (2007) 5251–5257.
[34] A. Tang, X. Wang, Z. Liu, Mater. Lett. 62 (2008) 1646–1648.
[35] W. Weppner, R.A. Huggins, J. Electrochem. Soc. 124 (1977) 1569–1578.
[36] X.H. Rui, N. Ding, J. Liu, C. Li, C.H. Chen, Electrochim. Acta 55 (2010) 2384–2390.